Demonstration of an HgCdTe Detector-Based Ultra-Stable Mid- Infrared Spectrometer for Transit Spectroscopy and Phase Curve Observations of Habitable Planets Around M-Stars

Technology Milestone White Paper
Proposal # 23-SAT23-0026

Johannes G. Staguhn[1,2] (PI),
Avi Mandell[2,] Dale Fixsen[2,3],Mario Cabrera[2], Craig McMurtry[4], Dan Kelly[2], Gregory Mosby[2], Peter Nagler [2], Edward Wollack[2]
[1]Johns Hopkins University [2]NASA Goddard Space Flight Center [3]CRESST 4University of Rochester, NY

May 13, 2025

Signature Page

E-SIGNED by
Johannes Staguhn, May 13, 2025

E-SIGNED by Johannes Staguhn
on 2025-05-13 17:49:00 GMT

Johannes Staguhn, Principal Investigator — Date
Johns Hopkins University

E-SIGNED by Nicholas Siegler
on 2025-05-13 17:49:19 GMT

Nick Siegler (ExEp Program Chief Technologist) — Date
Exoplanet Exploration Program, NASA/JPL –
California Institute of Technology

E-SIGNED by Brendan Crill
on 2025-05-13 17:47:00 GMT

Brendan Crill (Deputy ExEp Program Chief Technologist) — Date
Exoplanet Exploration Program, NASA/JPL –
California Institute of Technology

E-SIGNED by Lucas Paganini
on 2025-05-13 18:33:45 GMT

Lucas Paganini — Date
ExEp Executive, NASA-HQ

Table of Contents

1.0 Objective

This whitepaper describes the purpose and context of our planned work for NASA's Exoplanet Exploration Program (ExEP) within the NASA Strategic Astrophysics Technology (SAT) program. The stated goal is *to demonstrate and enhance the TRL of an ultra-stable HgCdTe detector-based mid-infrared spectrometer in combination with a high precision calibration scheme.* We describe the methodology for assessing the Technology Development for ExEP-SAT milestone metrics and establish the success criteria against which the milestone will be evaluated. The main milestone is the demonstration of *HgCdTe detectors* in an ultra-stable spectrometer, which, in a prior SAT, we successfully demonstrated with sub-K Transition Edge Sensor detectors to allow the extraction of mid-infrared spectral lines observed in the atmospheres of transiting planets around M-stars that potentially indicate the presence of life on the planet. As reference, transits of the habitable zones (HZ) planets around TRAPPIST-1 have a duration of ~2 hours, while phase-curve observations require observations over a few days. The required sensitivity for the detection of bio-signatures is typically 5 parts per million (ppm), which is not expected to be achievable with currently existing MIR spectrometers such as MIRI on JWST. Demonstration of a spectrometer with this precision and stability presents the required success criterion for having achieved the stated goal of the proposal.

2.0 Introduction

We have now detected many earth-size rocky planets in the *habitable zone* of their star – potentially pointing to an observational way to answer the question "Are we alone?". The habitable zone (HZ) is determined by incident radiation - but incident radiation is merely a proxy for surface temperature and the size of a planet is only a proxy for presumptive atmospheric pressure. Actual measurements of surface temperature and atmospheric conditions are required to confirm habitability, since the actual surface conditions will also depend on other factors such as initial composition, total lifetime UV flux, bombardment history, orbital stability, planet's magnetic field, etc. Mid-IR spectroscopic measurements of exoplanets allow actual temperature determination, as well as identifying atmospheric constituents and can reveal conditions necessary for habitability.

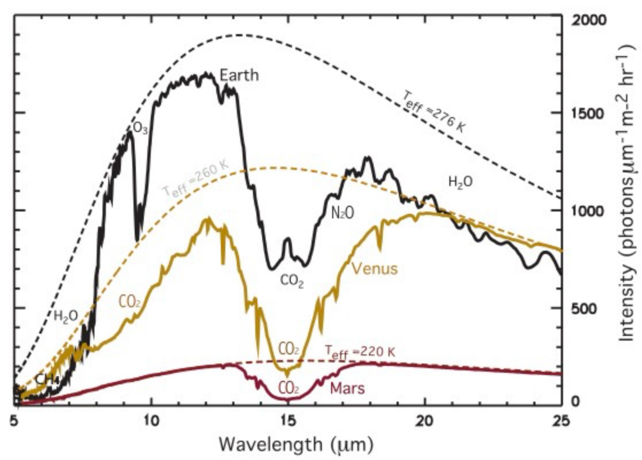

Figure 1. Relative intensity of planetary emission as a function of wavelength for three terrestrial planet models. The emission intensity for 300 K planets only rises at > 7 μm, and bands for ozone, carbon dioxide, nitrous oxide, and water vapor can all be readily observed at these wavelengths. Developing an ultra-stable spectrometer that can observe planetary emission from rocky habitable planets is critical to next-generation IR missions.

For terrestrial exoplanets in the habitable zones of mid-to-late M-dwarf stars, the planet-to-star flux contrast ratio becomes favorable at wavelengths > 5 μm (Figure 1), and the signal-to-noise ratio is favorable out to ~20 μm. Within the range from 5 μm to 17 μm, there are prominent absorption features from key markers of geological and biological activity, as well as the H_2O vapor continuum; these features can readily distinguish a wet Earth-like planet from a dry, Venus-like planet with a dense CO_2 atmosphere and a Mars-like planet with a thin CO_2 atmosphere. Additionally, emission spectroscopy uniquely probes a planet's thermal structure, and spectra from 5 μm and longer are less sensitive to high-altitude aerosols. Finally, thermal phase curves of tidally locked planets can probe the atmospheric and surface conditions as a function of longitude, providing a 2D map of a planet's surface and atmosphere.

2.1 RELEVANCE FOR FUTURE EXOPLANET MISSIONS

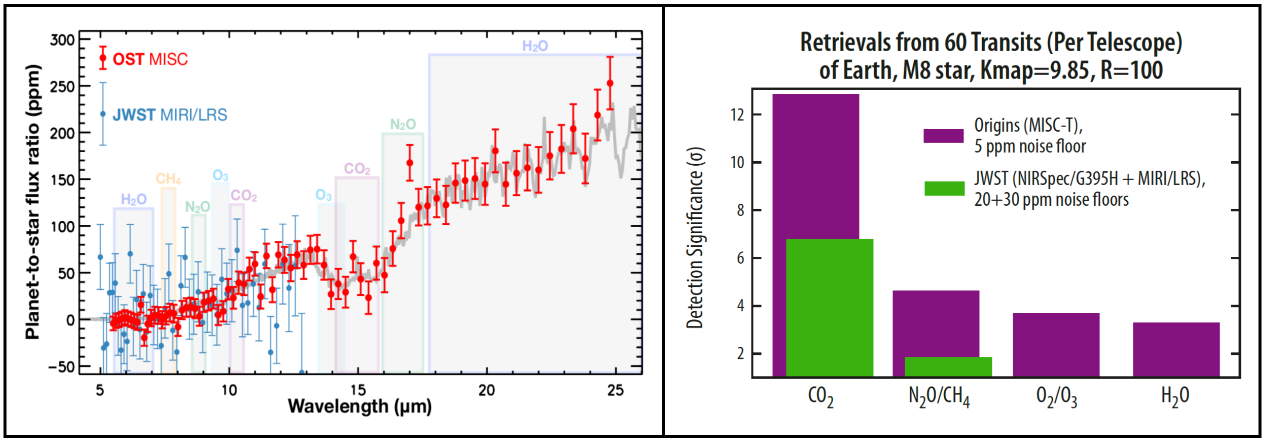

Figure 2. MIR spectral bands are critical for measuring the abundance of key constituents in atmospheres of terrestrial planets. An instrument like the Origins (OST) Mid Infrared Survey Camera-Terrestrial (MISC-T) transit spectrometer, spanning 5 – 18+ µm (left), would characterize habitable planets around nearby M-stars using the transit and secondary eclipse method. The detection of key constituents such as CO_2, N_2O and O_3 (right) and a measurement of the surface temperature will allow to determine whether the observed planets are habitable – but these measurements are only possible with an instrument such as MIRASET that can achieve a noise floor of 5 parts per million in the MIR.

Several future mission concepts aim to target thermal emission from habitable planets around M-stars. The *Origins* concept, studied for the Astro2020 Decadal Survey, included the MISC-T instrument which would be a mid-IR camera with integrated Transit Spectrometer for the detection of biosignatures in exoplanets in the habitable zone around M-dwarfs (Fig 2). Given its large aperture, broad wavelength coverage, and next generation instruments, *Origins* will be capable of efficiently characterizing a statistically significant sample of rocky planets, many of which will be in their host stars' habitable zones – as long as it can meet the noise floor requirement of 5 parts per million across the NIR and MIR.

Future Explorer and/or Probe concepts for dedicated MIR exoplanet spectroscopy missions will also benefit from this demonstration of an ultra-stable MIR spectrometer; for example, the MIRECLE mission (Staguhn et al. 2019b, Mandell et al. 2022, Staguhn et al. 2022) would utilize the same wavelength range but would focus solely on the nearest M-star systems using the Planetary Infrared Excess (PIE) technique to target both transiting and non-transiting exoplanets .MIRECLE would survey ~ 40 temperate rocky and sub-Neptune-mass planets around the nearest M-stars, determining which planets have atmospheres and show signs of habitability. **The same high-stability, broad-wavelength spectrometer is required for all these mission concepts – and our concept, we call the Mid-InfraRed Array Spectrometer for Exoplanet Transits (MIRASET), provides a high-TRL path to this goal.**

2.2 HG CD TE DETECTORS

Our previous version of MIRASET utilized a TES detector-based spectrometer and yielded the required sensitivities (Fixsen et al., 2025). However, the 0.1K temperature required to operate TES bolometers will be costly for a space mission. We are therefore proposing to utilize a recently developed and characterized MIR HgCdTe detector array, which requires a higher base temperature of ~24 K that would greatly reduce mission cost. Shorter wavelengths versions of these detectors have high heritage for space missions, including the readout technologies and their readout electronics (e.g. JWST). The measured values for the dark current of the long wavelength array (~30 $e^{-}, Cabrera$ 2020) and other detector characteristics would provide star-photon noise limited conditions for the majority of exo-planet mission designs and targets, and is discussed in more detail in Mandell et al., 2022. However, they have not been tested for the temporal stability necessary for transit spectroscopy measurements. This is what we are proposing to test, providing a necessary step towards enabling MIR exoplanet spectroscopy in space without the requirement for sub-K cooling.

HgCdTe detector array technology has matured over the years, where devices with a cutoff wavelength of 2.5 - 5 µm have been used for WISE, JWST and the upcoming Roman Space Telescope. The desirability of $Hg_{1-x}Cd_xTe$ (where x is the molar fraction of cadmium) detector arrays for astronomy is the tunable cutoff wavelength, with the added benefit that the operating temperature can be achieved for a space mission with passive cooling, unlike the cases for Si:As IBC and TES detector arrays. The bandgap energy as a function of x and temperature T of HgCdTe is given by Hansen and Schmidt, 1983 (empirically derived): $E_g(x,T) = -0.302 + 1.93x - 0.81x^2 + 0.832x^3 + 5.35 \times 10^{-4}T(1-2x)$, where higher mercury to cadmium ratio in the material will lead to longer cutoff wavelengths. The production of 20+ µm HgCdTe devices for astronomy may be possible, but the performance of longer cutoff devices may be limited by larger tunneling dark currents (Bacon, 2006; Kinch, 2014), and the softer material (due to increased mercury content) can lead to an increased likelihood of forming defects/dislocations (Carmody et al., 2003) that contribute to trap-assisted dark currents.

Recent results from a developmental project pursued by the University of Rochester (UR) infrared detector group and Teledyne Imaging Systems (TIS) to produce 15-µm cutoff HgCdTe detector arrays yielded very encouraging results (Cabrera, 2020) that address the potential limitations of increasing the cutoff wavelength to 20+ µm. Three devices were produced by TIS (with substantial input from UR) to reach the goal of ~15 µm wavelength cutoff devices that employed a proprietary design to mitigate quantum tunneling dark currents. That project yielded three devices with excellent read noise (~30 e^{-}/s), QE (>= 80% in the 6-12 µm wavelength range, without anti-reflective coating), and reduced expected tunneling dark current behavior. One of those three devices, H1RG-20302, has a cutoff wavelength of 16.7 µm at a temperature of 30 K and is bonded to a HAWAII-1RG Multiplexer.

The characterization of H1RG-20302 at UR showed that the performance of this device was limited by tunneling dark currents when a modest amount of reverse bias is applied to increase the pixel well depth (median well depth of 53 ke^{-} with an applied reverse bias of 350 mV) and could affect the noise of the device. Band-to-band tunneling dark currents (Sze, 1981) are the dominant source of dark current for biases > 180 mV, while combination of generation and recombination (G-R) trap-assisted thermal dark currents (Sah et al., 1957), trap-assisted quantum tunneling (Kinch, 1981), and a light leak the UR test dewar limited the dark current performance at lower biases (Figure 3). These results are very encouraging since the tunneling dark currents showed an improvement in the TIS proprietary design of this device by several orders of magnitude (Cabrera 2020). Additionally, this was the first attempt in producing these devices; with further enhancement to the device design, the tunneling currents may be conceivably mitigated further. The HAWAII mux was

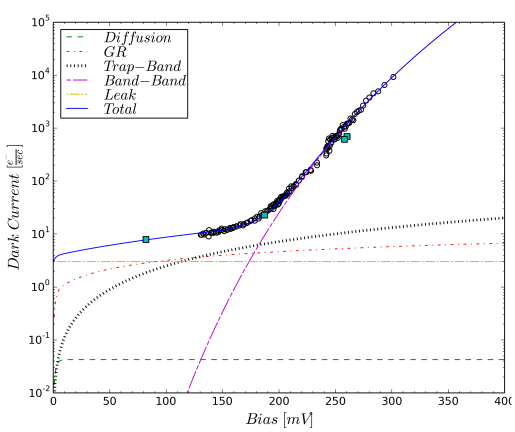

Figure 3. Dark current vs. bias (at 23 K). The cyan square data points show the initial dark current and detector bias for dark SUTR (Solid-State Ultraviolet-Visible Photodetectors)curves (see Cabrera 2020).

chosen by UR for the 15 µm devices due to their lower power dissipation relative to CTIA (capacitive trans-impedance amplifier) structure muxes, which is beneficial to both the detector temperature stability and thermal load on the cooler. We will control the temperature of the HgCdTe detector to 20 - 25 K to minimize the dark current, while maintaining the highest level of operability. Although the readout electronics are mature, the optimum settings for a colder, detector with extended range to ~18 um has not been explored. We will control the temperature of the HgCdTe detector to a target temperature between 20 and 25K while maintaining a stability of +/- 100 mK. This will permit us to ascertain the stability of the dark current in this region and determine the optimal temperature for best noise performance. In addition, since the longer wavelength H1RG devices have higher dark current than their shorter wavelength counterparts (Cabrera 2020), we will explore the impact of the trade space between frequent resets and higher full well on detector stability. This will allow us to determine the suitability of these devices for the intended observations. Another advantage is the maturity of the readout electronics for HxRGs. The rest of the system beyond the detector is already TRL-6+, thus investment in calibrator/detector has potentially a significant payoff for competed missions.

The long-term stability of HgCdTe detectors is critical for this demonstration. Recent results for the shorter wavelength NIRCam HgCdTe detectors on JWST are very promising in this respect, with an estimate from time stream measurements that indicates the total stability of the devices to be better than 9 ppm, which includes temperature fluctuations (Schlawin, et al., 2021). Without using PID temperature control for the detectors on JWST they are still subject to thermal variations. With PID temperature control down to better than 100mK (Staguhn et al., 2019a), we expect that MIRASET will be capable of demonstrating significantly better thermal stability, making it possible to reach our goal of 5 ppm. It is, however, not clear, whether those numbers will be straight-forwardly applicable to the long wavelength devices tested in this project. While we address all instrument and measurement -specific sources of noise, limitations due to astronomical sources such as variations in the stellar flux, which is being worked on in other theoretical work (e.g. Stevenson et al., 2020), are not being addressed in this study.

The potential for high stability, relatively warm operating temperatures that can be provided by passively cooled space platforms, and clear path to achieve a TRL of 5 make these new long-wavelength H1RG arrays a potentially ideal choice for a mid-IR exoplanet spectrometer used in this proposed project to test its stability during long integrations to determine if this technology would be suitable for *Origins*, MIRECLE, and other potential exoplanet mission concepts.

2.3 MID-IR SPECTROMETER TECHNOLOGIES

Instrument Key Attributes:

- Photon-noise limited performance
- High stability
- Sufficient dynamic range for Transit Spectroscopy
- Integrated high-precision calibration

Doped silicon impurity band detectors are currently used for Mid-IR astronomical instrumentation; however, these have significant stability issues as e.g. described in (Rieke et al., 2015). JWST MIRI transit observations (Bouwman et al. 2023) and phase curve observations (Kempton et al. 2023) show that MIRI's LRS noise floor is above 25 ppm. As a result, the achievable stability of those detectors will not allow for the detection of biosignatures in the atmospheres of Earth-like planets in the habitable zone of M-stars. The ACADIA readout system has flight heritage (Loose et al., 2018). Therefore, in this proposal we can focus on the performance of the HxRG devices and their calibration schemes: A calibration system is necessary, since there are no known infrared detectors that provide 5 ppm stability over many hours (Greene et al., 2016). Under a prior SAT (18-SAT18-0024), we have developed very stable, large format, high efficiency low noise TES-Transition Edge Sensor (TES) based bolometer arrays operating from the mid-infrared to submillimeter, wavelength regimes (Benford et al., 2010). The calibration scheme for *MIRASET* (described below) is independent of the detector used, and thus in this project we are going to demonstrate an existing long wavelength HgCdTe detector from the University of Rochester in a new dewar that uses the same parts of the existing spectrometer (but operates the detectors at above 20 K). We will test whether the required detector stability over many hours, needed for the detection of bio-signatures in the atmospheres of exoplanet through transit spectroscopy in the mid-IR can also be achieved with this detector.

Calibration system: We have developed a calibration system (Fig. 4), centered around a standard tungsten filament light bulb capable of heating its filament to 2500 K, closely resembling the spectrum of a typical M star. Monitoring this light bulb is an optical diode (Vishay BPW21R) equipped with a filter (ThorLabs 500FS80-12.5), allowing only visible light to reach the photo diode. These optical diodes offer intrinsic stability and leverage the visible spectrum, exploiting the exponential dependency of light on temperature in the Wien part compared to the nearly linear dependency in the Rayleigh-Jeans part. This results in a 7-8 times greater variation in optical output compared to the mid-infrared, where crucial observations are focused.

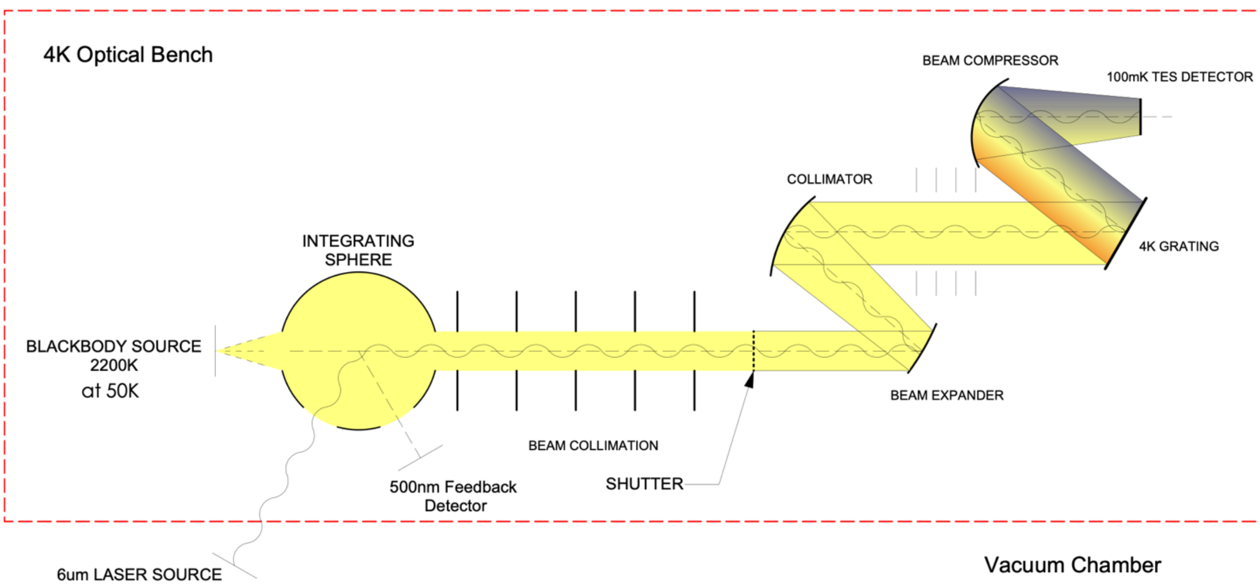

Figure 4. Schematic showing the existing MIRASET test bed in our lab. Most of the calibration system (integrating sphere and the photodiode for temperature monitoring) are all at 4 K together with the cold optics, mid-IR grating and are temperature controlled with a PID. The TES detector array at 100 mK. The black body source (light bulb) can be temperature controlled at the 50 K stage. The infrared laser is at 300 K. Note that the optical coupling of the laser will not be very sensitive to temperature fluctuations and that the laser only serves as frequency calibration. Amplitude variations in the laser output will not affect the accuracy of the calibration. Note that the new spectrometer configuration will be very similar, only that the 50 K stage will be replaced by a 100 K stage and the 4K stage will be operated at 20 K, which includes the detector base temperature.

Initially, a TES detector was selected for its demonstrated low 1/f noise. To maintain cost-effectiveness, a 9×9 TES detector was used instead of one optimized for the spectrometer, although only 33 of its 81 pixels were instrumented due to wire bonding limitations. This choice limits the observed spectrum to a small segment. While a more ideally shaped TES detector, such as an 8×64 configuration, could be manufactured, it exceeds the project budget.

To accommodate the detector's low-frequency variations, the light bulb must be switched on and off quickly yet being allowed to reach a steady state. Fortunately, there is a broad frequency range available for this in the 10-1000 mHz range.

Implementation of temperature control: Many of the fluctuations in both detector gain and offset stem from temperature variations in either the detector or the electronics. To manage these temperature fluctuations, a thermometer is attached to the detector and at each individual temperature stage. The thermometer readout can be interfaced with a PID (Proportional-Integral-Derivative control loop)-controlled heater which will be integrated into the detector package.

Cryostat: We will equip an existing cryostat incorporating a high power 2-stage cryocooler (using an existing compressor). The outer segments of the cryostat will be heat sunk to the first stage of the cooler which is at 100 K. The cold stage of the cryocooler is at 20 K, being an ideal 5 K below the optimal detector temperature around 25 K (the temperature difference allows for efficient PID-ing). To handle its relatively high power and have it thermally separated from the detector stage, the light bulb will be affixed to the 100 K stage. The ACADIA readout system will also be mounted to the 100 K stage. Since we plan to PID temperature control this stage, we will be able to provide valuable information for Roman on the benefits on temperature controlling the ACADIA. The integrating sphere, spectrometer, and optical diode will be affixed to the 20 K stage.

Test Results from our prior SAT demonstration using TES detectors:

We describe the results of our prior demonstration of MIRASET equipped with TES detectors in order to illustrate the planned measurements with the HgCdTe detectors, since those will be nearly identical:

The light bulb, stripped of its glass cover, received excitation from a 100 mHz frequency sine wave, illuminating the TES detector via an integrating sphere. Ten pixels of the TES detector were sampled at a rate of 4 kHz. Thermometers were strategically positioned throughout the cryostat to monitor temperatures, including those of the 50 K stage, the 3 K cold head, the spectrometer/photo diode and integrating sphere, and the detector itself. These thermometers were sampled at 1 Hz, while the readout of the photo diode was sampled at 32 Hz. The light bulb's modulation occurred at a relatively slow rate, allowing for 320 samples per cycle of the photo diode. Figure 5 illustrates typical data captured from one of the TES pixels, with the remaining pixels exhibiting similar patterns. It is worth noting that the light bulb's driving signal was a sine wave. However, the resulting mid-IR signal deviates from a pure sine wave due to the light bulb's nonlinearity and the shifting color temperature as the light bulb heats and cools. The sine wave repetition occurs 2200 times over a span of 6 hours.

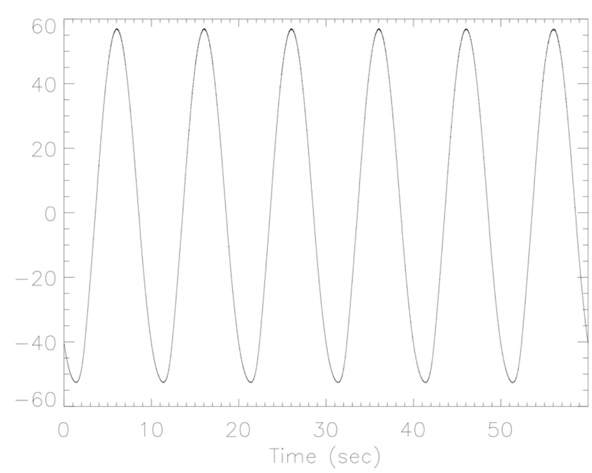

Figure 5. Raw data captured from one of the TES pixels. The readout signal is dominated by the sine-modulated light bulb.

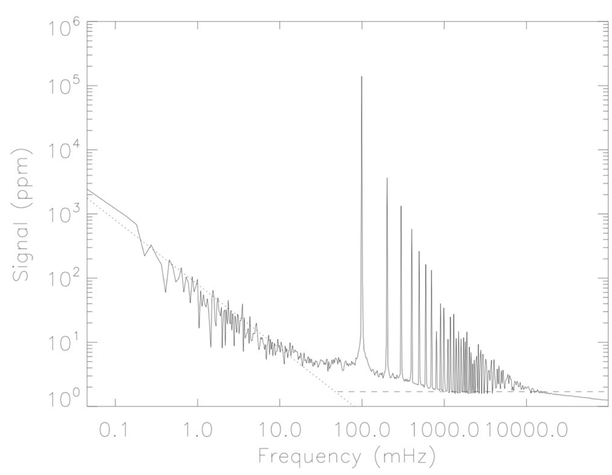

Figure 6. Power Spectrum of one Pixel. Peak has been suppressed by logarithmic binning. Note 1/f low frequency noise (dotted line). White noise is approximated by dashed line.

.

In Figure 6, a power spectrum derived from one of the pixel readouts is shown, smoothed using logarithmic binning. This spectrum is normalized to the amplitude of the 100 mHz signal emitted by the light bulb. The presence of numerous spikes at harmonics of 100 mHz demonstrates a more intricate response from both the light bulb and the TES detector than expected from a simple sine wave. This is due to the temperature change of the filament during switching, which results in the response function deviating from a pure sine shape. Also noticeable is the high-frequency white noise floor and the low-frequency rise, approximately following a $1/f^{0.9}$ trend. The knee frequency is around 45 mHz.

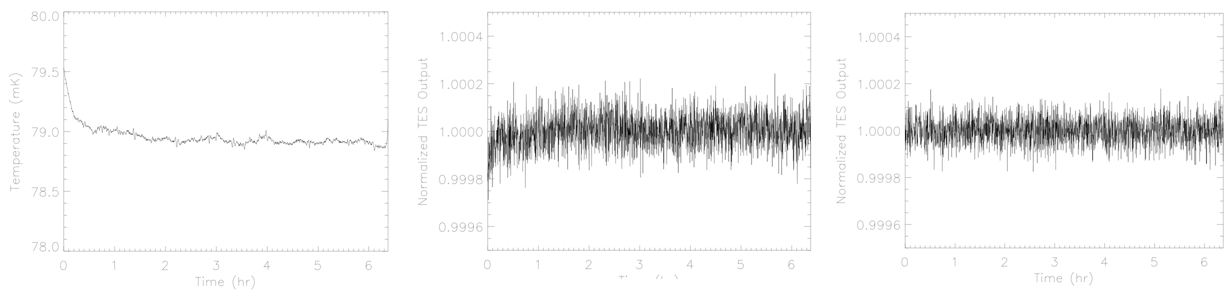

Figure 7. *left:* Detector package temperature; *center*: Raw gain response of one Pixel. Signal has been normalized so the average is one; *right:* Gain response after correction for temperature drift and common mode removal.

Figure 7 (left) shows the temperature of the detector package throughout the 7-hour experiment. The average temperature recorded during the experiment is 79 mK, with a root mean square (RMS) variation of 83 μK. The fluctuations in temperature exhibit a noticeable correlation with the fluctuations in the TES (Transition Edge Sensor) readout. However, the primary variation observed pertains to the gain rather than the offset. The modulation effectively eliminates the offset, revealing that the gain remains more consistently stable in comparison. For the purpose of using the temperature data for data processing we blanked out the data of the first 20-30 minutes, where the temperature is still settling. The data then were de-modulated using the measured modulation curve of light bulb. Figure 7 (center) shows the normalized amplitude of the detector readout. Figure 7 (right) shows the same, but after subtraction of the measured thermal drifts plus the measured common mode of all pixels.

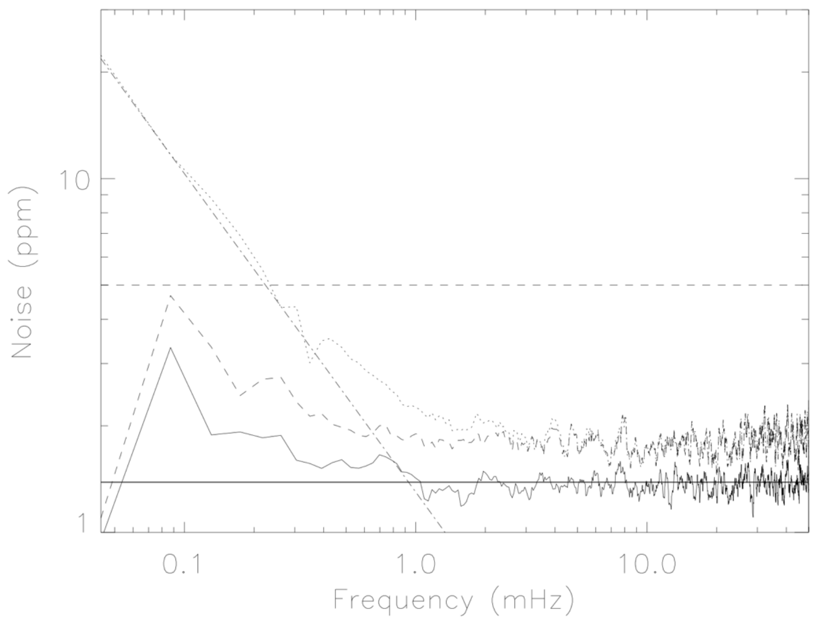

Figure 8. Average Spectra for raw data (dotted line), with temperature variation removed (dashed line) and with common mode removed (solid line). Dashed horizontal line is 5 ppm the goal of this experiment. The dash-dot diagonal line is a $f^{-.9}$ approximation to the low frequency noise. The solid horizontal line is a fit (1.385 ppm) to the white noise in the common mode rejected fit.

Figure 8 shows the demodulated spectral noise density plot for one data set, going down to (~7 hours). One can see that for the demodulated, temperature and common mode corrected data (solid line in the figure) the experimental requirement of a stability of < 5 ppm is still met for 7 hours of data acquisition.

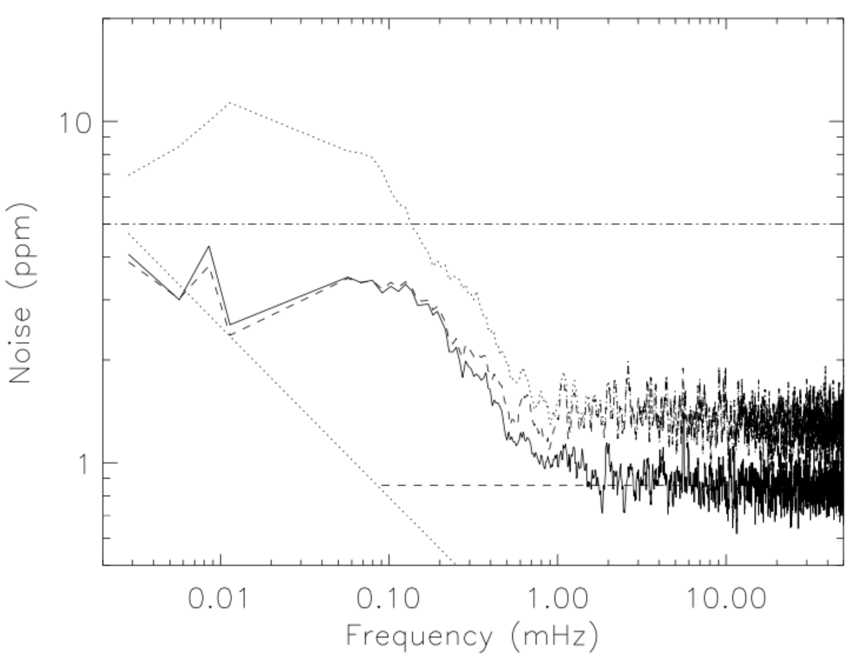

Figure 9. Average Spectra of four sets of concatenated raw data (dotted line), with temperature variation removed (dashed line) and with common mode removed (solid line). Dash-dot horizontal

line is 5 ppm the goal of this experiment. The dotted diagonal line is a 1/√f approximation to the low frequency noise. The dashed horizontal line is a fit (.85 ppm) to the white noise in the common mode rejected fit.

Lastly, we coadded several data sets to measure the noise floor out to four individual measurements, lasting about 7 hours each and taken over 4 days which we coadded into one dataset (Fig. 9). This is the same method as will be the case to add phase curve data over several days. Still, the stability requirement of 5 ppm is still met in this data set, which we describe in more details in Fixsen et al., 2025.

.

2.4 DIFFERENCES BETWEEN FLIGHT AND LABORATORY DEMONSTRATIONS

The optical configuration in the lab is obviously different, since the BB radiation and the "source signal" (laser) get combined in the instrument's sphere, whereas in space the source (star plus planet) enters through the primary while we intend to mix it with the BB radiation at the position of the secondary mirror of the telescope. This will ensure that both share most of the optical train in the observatory.

At L2 the flight environment will be more stable than the laboratory environment. First at L2 there is no diurnal cycle making the thermal environment much more stable. There is no vibration except those introduced by the spacecraft itself meaning the mechanical environment is much more stable. Finally, L2 is far away from cell phones and other radiofrequency electrical interference.

Radiation tests of the HgCdTe detector will be necessary to achieve TRL 5.
While not a necessary deliverable for this grant, we will strive to obtain those or at least provide an analysis of how radiation tests of existing shorter wavelengths HgCdTe detectors used in existing mission can be used for verification.

3.0 Milestones and Success Criteria

Demonstrate gain stability of 5ppm over 4 hours up to 4 days, of a mid-IR transit spectrometer with a 17μm-cutoff HgCdTe detector.

3.1 MEASUREMENT OF THE EXO-PLANET

The spectrometer is designed to provide unprecedented stability, enabling the currently unachievable goal of characterizing exo-planet atmospheric lines that are strong indicators for the presence of life.

The scientific product provided by the spectrometer will be the measurement of the planet's transmission and/or emission spectrum. The measured spectrum is dominated by the BB emission from the star. Superimposed on this BB radiation will be the spectral features due to atmospheric lines, which can be in emission or absorption. Examples include O_3, CO, H_2O, and the biosignature tracers NH_3 N_2O, if found in co-existence with O_3. This "small signal" from the planet is on top of the star's significantly stronger emission and will need to be cleanly separated, resulting in the stated goal for the precision of this measurement of 5 parts per million (ppm), which is achieved by monitoring a modulated black body source (modulation frequency 0.1 Hz) with integration times ranging from over ~ 4 hours, to 4 days. Other, than the prior successful demonstration using Transition Edge Sensors (Fixsen et al., 2025), the 4-day measurements will be obtained without

gaps, since continuous cooling at 24 K is provided. The stated 5 ppm precision corresponds to the ratio of the measured signal strength and the amplitude of the spectral power noise density over all ranges of frequencies from 3 μHz (corresponding to 4 days) up to the readout frequency of a few Hz.
A major source of 1/f noise in detector readout data are temperature fluctuations. I our demonstration of the proposed spectrometer with Transition Edge Sensors, we indeed found the major 1/f noise contribution to come from temperature fluctuations (Fixsen et al., 2025). Just using the measured temperature variations and using those for the common mode subtraction from the data was sufficient to achieve the 5 ppm goal, i.e. active temperature control was not even necessary to meet the requirements. Nevertheless, we plan actively control temperatures this time, since by now we have obtained and developed all necessary hardware- and firmware tools for this.

3.2 MILESTONE DEMONSTRATION PROCEDURE

The requirement is 5 ppm stability in the instrument measurement capability. The stability will be mostly affected by: 1. instrument's temperature stability. 2. detector stability 3. black body source (BB) stability. 4. optical stability, which is dominated by the mechanical robustness of the instrument. However, with virtually no long-term stability measurements of HgCdTe detectors, we do not quantitatively know the individual contributions of those elements. Consequently, one of the goals is to find out which of the elements is critical as that will be the one dominating the error budget. The following milestones will be achieved during this project:

- 100 K detector cooling stage temperature stability demonstration (with and w/o feedback control)

We will measure the open loop temperature stability of the 100 K stage temperature and derive the response of the ACADIA readout electronics to those. We will PID the stage.

- 20 K detector cooling stage temperature stability demonstration (with and w/o feedback control)

a) We will measure the open loop temperature stability of the 20 K detector cooling stage temperature.

b) Once the detectors have been installed and verified in the spectrometer, we will measure the temperature to readout conversion factor by measuring the detector response to temperature variations in the 20 Kbase temperature. If necessary, stability requirements for the 20 K stage control will be adjusted accordingly.

- Measurement of the Black Body (BB) temperature stability with and without feedback control
In this step we measure the BB stability with the photo-diode with and without PID control. We will verify that the required sensitivity of the measurement will be achieved in the predicted amount of integration time to verify our prediction for the achievable signal to noise (s/n) ratio.
We will show that we can stabilize the temperature of the tungsten filament to within a few mK at 2200 K. We will also show that we can switch between a couple of temperatures e.g. 2100 and 2300 K reliably within a minute or so.

- Measurement of BB curve and spectral stability thereof
Once the frequency stability of the laser has been quantified we will determine the "broader" frequency stability by fitting the correct BB SED to the measured BB temperature. Any residuals measured will be used to quantify broader (i.e. correlated over two or more spectral pixels) gain

variations. This demonstration instrument will not have the full frequency capability so the limits on the black body curve temperature will not be as stringent as the other limits, but will still be good to a small fraction of 1%.

- Verification of overall stability in measurement over days

The final instrument characterization will be a combination of all measurements described above, taken over the duration of several days in order to quantify the long-term stability of the system. When the system is run over several successive nights, we will measure the stability of the instrument and the reproducibility of the gain and offset from one night to the next to a few ppm.

3.3 SUCCESS CRITERIA: STABILITY ACHIEVED FOR THESE MEASUREMENTS

Success criteria for our lab spectrometer performance are straightforward: demonstration of the spectrometer stability to 5 ppm over 2 hours, which is required for the Trappist-1 HZ planets, and over days, needed for the phase curve observations of non-transiting planets. If we can show that this stability can be obtained over the entire band, we do not need to do a more sophisticated analysis of the data. However, even if there are still residual common-mode gain- and offset variations in the data, demonstration of successful removal of those, still obtaining a spectral accuracy, which can be demonstrated on the laser spectral lines in the lab setup will be required. Obviously, the very challenging stability requirement will only be demonstrable, if the laser itself is stable to within those limits, as well as the BB source, or the accuracy of the knowledge of its temperature. In order to provide this, we will temperature control the laser and the base plate of the BB source.

3.4 SCHEDULE NARRATIVE

January 2025 – June 2025:

- Dewar Design (using an existing dewar shell)
- Purchase necessary components (Cryo Cooler Head, mechanical and optical parts, including detector mount, spectrometer, Black body mount, black body light tubes, thermometers, ACADIA cold readout electronics, warm readout box, thermometry box, computer connections (fibers, USB cables), etc.
- Develop/modify software for thermometry and data readout. Modify firmware for H1RG readout.
- Delivery readout electronics (from Goddard collaborators) and detector package (from Rochester collaborator).
- Begin assembly of system

July 2025 – December 2025:

- Finish System Assembly
- Test dewar and components
- Test detector readout
- Bug fixes
- Prepare for milestone demonstrations as outlined in section 3

January 2026– June 2026:

- Milestone demonstrations
- Data analysis/interpretation
- If necessary, adjust experimental setup

July 2026 – December 2026:

- Finish milestone demonstrations
- Writeup results
- Publish results

4.0 References and Citations

Bacon, C.M., 2006, PhD Thesis, University of Rochester

Benford, D.J., et al., 2010, SPIE, 7741, 77411

Bouwman, J. et al., 2023PASP, 135c, 8002B

Cabrera, M. S., 2020, PhD thesis, University of Rochester

Cabrera, M. et al., 2019 Journal of Astronomical Telescopes, Instruments, and Systems, 5, 1

Charbonneau, D., et al. 2002, ApJ, 568, 377

Carmody, M. et al., 2003, J. Electron. Materials, 32(7), 710–716

De Wit, J., et. al 2016, Nature, 537, 69

do Amaral, L., et al. 2022, ApJ, 928, 12

Dressing & Charbonneau, 2015, ApJ, 807, 45

Dittman, J., et al. 2017, Nature, 544, 333

Fixsen et al., *Rev. Sci. Instrum.* 96, 023101 (2025). https://doi.org/10.1063/5.0234253

Fauchez, T., et al. 2019, ApJ, 887, 194

Gillon, M., et al. 2017, Nature, 542, 456

Greene, T., et al., 2016, The ApJ, 817,17

Greene, T., et al. 2023, Nature, 618, 39

Hansen, G.L. and Schmit, J. L , 1983, J. Appl. Phys. 54(3), 1639–1640

Kempton, E., et al. 2023, Nature, 620, 67

Kinch, M. A., 2014, State-of-the-Art Infrared Detector Technology, SPIE Press, Bellingham, Washington

Kinch, M., 1981, Semicond. Semimetals 18, 313–378

Kreidberg, L., et al. ApJ, 793, L27

Line, M., et al. 2016, ApJ, 820, 78

Loose, M. et al., Proceedings of the SPIE, 10709, 18

Mandell, A., et al., 2022, AJ, 164, 176M

Mennesson, B., et al. 2020, SPIE, 11443, 20

Mulders, G. et al., 2015,ApJ, 814, 130

Pascucci, I., et al. ApJ, 831, 125

Rieke, G., et al., 2015, PASP, 127, 665

Roberge, A., & Moustakas, L. A. 2018, Nature Astronomy, 2, 605

Sabotta, S., et al., 2021, A&A, 653, A114
Sah, C.T., Noyce, R.N. and Shockley, W., 1957, Proc. IRE 45(9), 1228–1243

Scalo, J., et al. 2007, Astrobiology, 7, 85

Schlawin, E. et al., 2021, ApJ, 161, 115

Shields, A., et al. 2016, Phys Reports, 663, 1

Staguhn, J., et al., 2019a, IEEE Aerospace Conference, Big Sky, MT, USA, 2019, pp. 1-10

Staguhn, J., et al., 2019b, Astro2020: Decadal Survey on Astronomy and Astrophysics, APC white papers, no. 238, Bibcode: 2019, BAAS, 51g, 238S

Staguhn, J., et al., 2022, SPIE, Volume 12180, id. 121802Q

Stevenson, K. B. 2020, ApJL, 898, L35

Stevenson, K., et al. 2014, Science, 346, 838

Sze, S.M., 1957, Physics of Semiconductor Devices, John Wiley & Sons, New York

Tarter, J., et al. 2007, Astrobiology, 7, 30

Valente, E., & Correia, A. A&A, 665, A130

Zieba, S., et al. 2023, Nature, 620, 746